AUTOPHAGY
2020, VOL. 16, NO. 12, 2167–2179
https://doi.org/10.1080/15548627.2020.1719681

Taylor & Francis
Taylor & Francis Group

RESEARCH PAPER

A new transcription factor ATG10S activates IFNL2 transcription by binding at an IRF1 site in HepG2 cells

Miao-Qing Zhang[a,b,c], Qiong Zhao[a], and Jing-Pu Zhang[a]

[a]Key Laboratory of Biotechnology of Antibiotics, the National Health Commission (NHC), Beijing Key Laboratory of Antimicrobial Agents, Institute of Medicinal Biotechnology, Chinese Academy of Medical Sciences and Peking Union Medical College, Beijing, China; [b]Postdoctoral Scientific Research Workstation, China Resources Sanjiu Medical & Pharmaceutical Co., Ltd., Shenzhen, China; [c]Postdoctoral Mobile Research Station, Institute of Process Engineering, Chinese Academy of Sciences, Beijing, China

ABSTRACT

IFNL2 is a potent antiviral interferon, but the regulation of its gene expression is not fully clear. Here, we report the regulation of ATG10S for *IFNL2* transcription. Through sequential deletion of the *IFNL2* promoter sequence, we found *LP1-1*, a fragment of the promoter responding to ATG10S activity. Subcellular localization and DNA immunoprecipitation assays showed ATG10S translocating into the nucleus and binding to *LP1-1*. Online prediction for transcription factor binding sites showed an IRF1 targeting locus in *LP1-1*. Luciferase assays, RT-PCR, and western blot analysis revealed a core motif (CAAGAC) existing in *LP1-1*, which determined ATG10S and IRF1 activity; individual nucleotide substitution showed that the functional nucleotides of ATG10S targeting were C1, A3, and C6, and the ones associated with IRF1 were A3 and G4 within the core motif. Co-immunoprecipitation assays revealed ATG10S combination with KPNA1/importin α, KPNB1/importin β, and IRF1. The knockdown of endogenous IRF1 increased ATG10S activity on *IFNL2* transcription. These results indicate that ATG10S as a transcription factor competes with IRF1 for the same binding site to promote *IFNL2* gene transcription.

Abbreviations: ATG10: autophagy related 10; ATG10S: the shorter isoform of autophagy related 10; BD: binding domain; CM: core motif; co-IP: co-immunoprecipitation; GFP: green fluorescent protein; HCV: hepatitis C virus; IF: immunofluorescence; IFN: interferon; IRF: interferon regulatory factor; LP: lambda promoter; MAP1LC3B/LC3B: microtubule associated protein 1 light chain 3 beta; RLU: relative light unit; SQSTM1: sequestosome 1.

ARTICLE HISTORY
Received 2 May 2019
Revised 14 January 2020
Accepted 17 January 2020

KEYWORDS
ATG10S; core motif; functional nucleotides; *IFNL2* promoter; *IFNL2* transcription; IRF1

Introduction

Type III interferons (also known as IFNLs/IFN-lambda/IFN-λs) are novel members of the IFN family and include IFNL1/IL29, IFNL2/IL28A, and IFNL3/IL28B [1]. Type III IFN proteins share a high degree of homology; IFNL2 protein shares 96% sequence homology with IFNL3 and 81% sequence with IFNL1 [2], indicating that a set of similar regulatory factors might dictate the expression of these IFNL genes. IFNLs are potent antiviral cytokines [3–5]. Virus replication can induce the expression of type I (IFNA2/IFN-α and IFNB1/IFN-β) and type III IFN genes via toll-like receptor (TLR)-dependent and TLR-independent pathways [6,7]. Although IFNL differs genetically from IFNA2 and IFNB1, they have similar biological antiviral functions with fewer side effects due to its receptor restriction [8]. Scientific research has shown that IFNL promotes the expression of IFN-stimulated genes (ISGs) via the JAK-STAT signaling pathway and induces the antiviral response [9]. *IFNL* gene promoters have various IFN-stimulated response elements (ISREs) and transcription factor-binding sites [10]. However, the interaction between *IFNL* gene promoters and multiple regulators is not fully clear.

Previous studies have shown that the interferon regulatory factor (IRF) family is a group of transcription factors that activates *IFN* gene transcription, which plays critical roles in the regulation of innate and acquired immune responses [11–13]. Each member of the IRF family contains a conserved N-terminal DNA-binding domain (BD), which recognizes the ISRE and promotes the transcription of ISGs [11,14–17]. Viral infection can induce the phosphorylation of IRFs at the C-terminal end and activated IRFs translocation into the nucleus, resulting in the expression of ISGs and IFNs [18]. The binding of IRFs to *IFNL* promoter ISRE sites is a critical event for the regulation of *IFNL* gene expression [10]. To date, the IRF family comprises at least nine members, namely, IRF1-IRF9 [19,20]. The regulation of type III IFN gene expression has been a subject of debate. IRF1 as an IFN-regulated gene (IRG) is involved in IFN-induced antiviral immunity and induces the expression of multiple IRGs such as IFNG/IFN-γ [21], IFNL/IFN-λ [22], TLR3 [23], and ISG20 [24]. IRF1 interacts with IFN-sensitive genes and other transcription factors via binding to the *IFN* promoter regulatory domain. In recent years, an increasing number of reports have indicated that IRF1 plays a crucial role in antiviral activity [25]; however, the mechanism is not well understood.

CONTACT Jing-Pu Zhang zjp5577@126.com Key Laboratory of Biotechnology of Antibiotics, the National Health Commission (NHC), Beijing Key Laboratory of Antimicrobial Agents, Institute of Medicinal Biotechnology, Chinese Academy of Medical Sciences and Peking Union Medical College, Beijing 100050, China
Supplemental data for this article can be accessed here.

Recently, the host homeostasis system and host restriction factor related to pathogen invasion have received extensive attention. Macroautophagy/autophagy and innate immunology are two of host homeostasis and defense mechanisms; cooperation between the two mechanisms constructs the host defense network [26]. Autophagy is a catabolic process that is important for maintaining cellular homeostasis [27] and resisting foreign pathogens together with the immune system [28,29]. Our previous study showed differential function between 2 isoforms of ATG10 (autophagy related 10) protein, ATG10 (longer isoform), and ATG10S (shorter isoform). Canonical ATG10 as an E2-like enzyme is involved in the conformation of the ATG12–ATG5-ATG16L1 complex, which promotes extension of the phagophore membrane and formation of autophagic vesicles. ATG10S activates expression of innate immunity-related genes, including IFNL2, and promotes complete autophagy by driving autophagosomes to interact with lysosomes via IFNL2 mediation, in which lysosomal dissolution degrades hepatitis C virus (HCV) subreplicons [28,30]. Surprisingly, ATG10S also translocates into the nucleus and combines with the *IFNL2* promoter [30]. These results raise the possibility that ATG10S might act as a latent transcription factor to promote the expression of innate immunity-related genes; however, the mechanism of ATG10S nuclear transport and the mechanism and functional sites for ATG10S in activating *IFNL2* transcription remains unknown.

As a follow-up to our previous study, we investigated these questions. This study also revealed the link between autophagy and immunity, and it showed the regulatory network of synergistic action between intracellular homeostasis and defense mechanisms. The results of this study also provide novel drug targets for the research and development of new antiviral strategies.

Results

Identification of the ATG10S-binding site on the IFNL2 *promoter*

First, we determined whether endogenous *IFNL2* transcription could be driven by ATG10S or IRF1 using gene overexpression and gene knockdown. The results indicate that, compared to the control group, ATG10S or IRF1 overexpression significantly raised endogenous IFNL2 levels, and *IRF1*-siRNA transfection decreased endogenous IFNL2 levels in transcription and translation, but ATG10 did not (Figure 1A). From this, we infer that both ATG10S and IRF1 function in the activation of *IFNL2* expression. Then, we began to search the detail loci for ATG10S and IRF1 binding on the *IFNL2* promoter. According to the GenBank NCBI Reference on the human *IFNL2* gene upstream sequence (homo sapiens chromosome 19, GRCh37.p5, NC_000019.9|:39752520–39759213), we designed two pairs of primers for cloning *IFNL2* 5′ upstream of the 2.1 kb sequence (Figure 1B). The function of the 2.1 kb fragment was primarily analyzed by ligating it into a green fluorescent protein (GFP) expression vector as lambda promoter-1 (*LP1*) and *LP2*, both of which could guide GFP expression in HepG2 human liver cancer cells under ATG10S overexpression (Figure 1B). The data showed that the *LP1* sequence was the functional *IFNL2* promoter fragment. The *LP1* sequence was cloned into the pGL3-basic vector with the luciferase gene as the reporter. The results revealed that the luciferase activity was noticeably increased with *LP1* as the promoter under ATG10S overexpression (Figure 1C). Simultaneously, RT-PCR and western blotting experiments showed that expression of GFP guided by *LP1* was also significantly enhanced under ATG10S overexpression, whereas ATG10 did not show these effects (Figure 1D). These results verified that *IFNL2* gene transcription induced by ATG10S is dependent on sequences within the *LP1* region. We searched the 1053 bases of the *LP1* sequence to identify the ATG10S-binding site. We divided the *LP1* sequence into three fragments, *LP1-1* (407 bp), *LP1-2* (404 bp), and *LP1-3* (373 bp), from the 5′ to 3′ end, and separately ligated these fragments into the pEGFP-ΔCMV-N1 vector from which the CMV promoter sequence had been deleted, forming three GFP-expressing plasmids guided by each fragment of the *IFNL2* sequence (Figure 1E). Subsequently, the constructs were separately co-transfected with 5′-capped mRNAs of *ATG10* or *ATG10S*, and RT-PCR and western blot results showed that ATG10S could promote GFP overexpression guided by *LP1-1*, but not by *LP1-2* or *LP1-3* (Figure 1F). Therefore, we inferred that the functional site is within the 407 bp sequence of *LP1-1*.

ATG10S functional site for the transcriptional activation of IFNL2 *is within the IRF1 transcription factor binding domain*

In recent years, accumulating evidence has revealed that IRFs are involved in promoting the expression of type III IFNs. We predicted the potential transcription factor binding domain (BD) of IRF1 in the 1 kb upstream sequence of the *IFNL2* gene by using the online prediction software JASPAR (*http://jaspar.genereg.net/*), which showed only one IRF1-binding site with a high score located in the *LP1* region (Table 1). Meanwhile, we found that the binding site of IRF1 was mainly in the *LP1-1* region and encompassed a 36-oligonucleotide region (Figure 2A). The above results suggested that ATG10S pro-transcription activity was also in this region; therefore, we explored whether the functional site of ATG10S binding to the *IFNL2* promoter was also related to the IRF1-BD. To this end, we used the BD-deleted *LP1-1* sequence as a promoter to construct two expression vectors, namely, pIFNL2ΔBD-EGFP with GFP as the reporter gene and pIFNL2ΔBD-LUC with luciferase as the reporter gene (Figure 2A). RT-PCR and western blotting showed that ATG10S did not promote GFP overexpression and did not enhance the luciferase activity, but it moderately reduced reporter expression in the *LP1-1-ΔBD* group compared with *LP1-1* (Figure 2B and C). The results indicated that the BD sequence was indispensable for ATG10S action on *IFNL2* gene transcription. We further divided the 36 bp sequence into 3 equal parts (unit 1, unit 2, and unit 3). Using sequential deletion of the 3 parts from the 5′ end, we produced four *LP1-1* deletion mutants: *BDΔ1, BDΔ1-2, BDΔ2-3*, and *BDΔ3*. Then we recombined the four deletion mutants upstream of the reporter genes in the pEGFP-ΔCMV-N1 and pGL3-basic vectors (Figure 2A). RT-PCR, western blotting, and luciferase activity assays revealed that in the *BDΔ1* and *BDΔ3* groups, GFP expression and luciferase activity were markedly increased by ATG10S and not by ATG10, similar to the *LP1-1* group. The other two deletions of *BDΔ1-2* and *BDΔ2-3* suppressed the action of ATG10S on *LP1-1* (Figure 2D–F). As shown in Figure 2A, *BDΔ1-2* and *BDΔ2-3* shared a common oligonucleotide

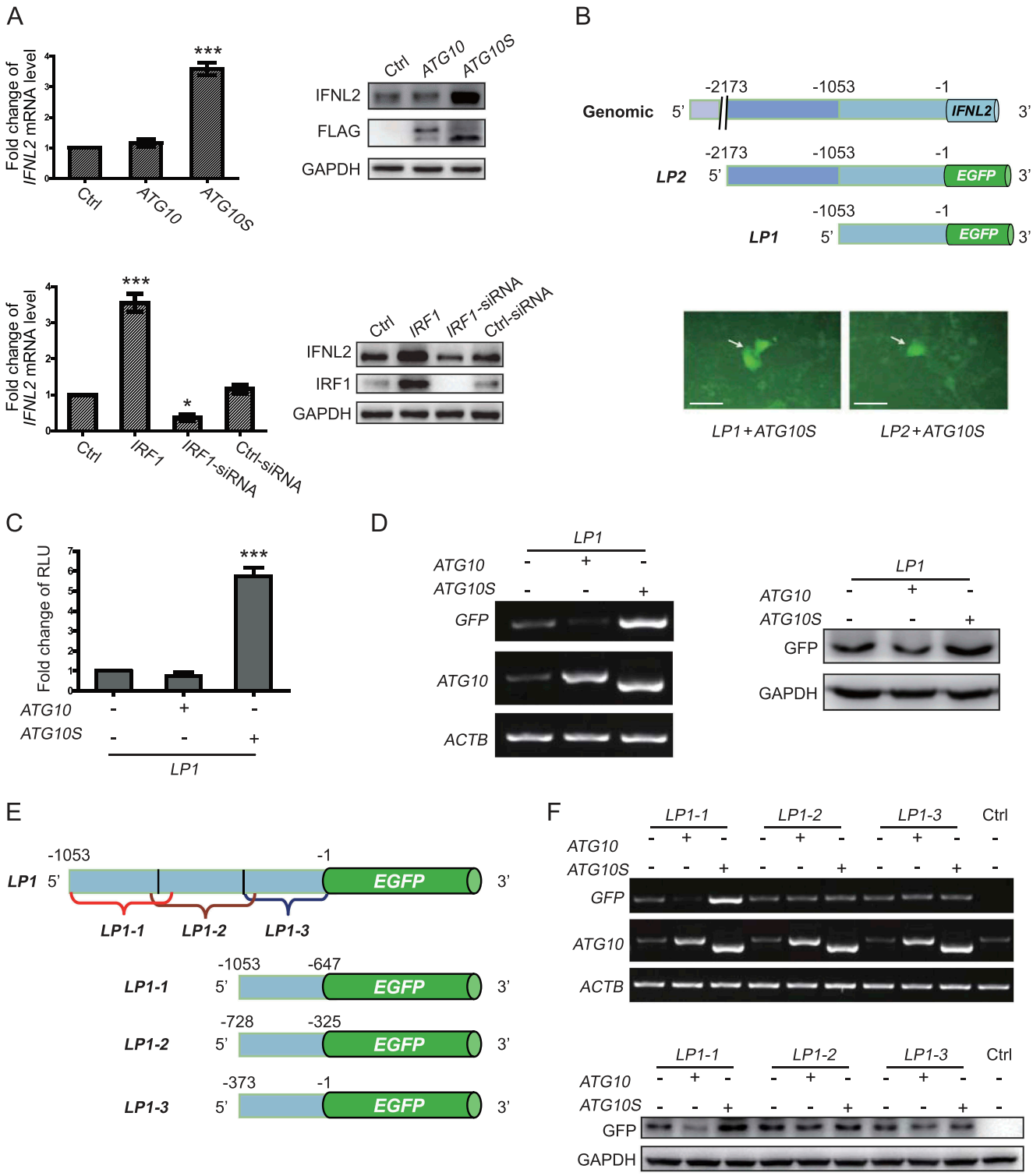

Figure 1. Potential ATG10S binding sites on the human *IFNL2* promoter within a 1 kb sequence from the initiation codon. (A) Endogenous IFNL2 expression levels in HepG2 cells were detected using qRT-PCR (left) and immunoblot assay (right) through the regulation of *ATG10S* and *IRF1* gene expression. ATG10 or ATG10S overexpression was achieved by transfection of plasmids with FLAG-tagged *ATG10* or *ATG10S*; IRF1 overexpression and knockdown were through transfection of *IRF1* 5′-capped mRNA and *IRF1*-siRNA respectively. Ctrl, non-transfection. Ctrl-siRNA, Control-siRNA. (B) Diagrams show the 2.1-kb genomic sequence of the *IFNL2* promoter, 2 expression constructs directed by *LP1* and *LP2* segments (upper), and fluorescence microscopy images for GFP expression directed by the *IFNL2* promoter fragments *LP1* or *LP2* induced by ATG10S in HepG2 cells (bottom). Scale bars: 220 μm. (C) Luciferase activity assay shows the different actions of ATG10 and ATG10S on *IFNL2 LP1* transcription activity. RLU, relative light unit. (D) RT-PCR (left) and western blotting (right) examined ATG10- and ATG10S-mediated activation of the *IFNL2 LP1* promoter. (E) Diagram of 3 *GFP*-expressing constructs directed by *LP1* truncated segments (*LP1-1*, *LP1-2*, and *LP1-3*). (F) RT-PCR (upper panel) and western blot (bottom panel) were used to determine the effects of ATG10 and ATG10S on GFP expression directed by the *LP1-1*, *LP1-2* or *LP1-3* segments respectively. Ctrl, non-transfection; * indicates $P < 0.05$, *** indicates $P < 0.001$. The statistics data are expressed as the mean ± standard deviation (SD) (n = 3).

Table 1. Prediction of transcription factor IRF1 BD on *IFNL2* 5′-upstream sequence *LP1*.

Model ID	Model name	Score	Relative score	Start	End	Strand	predicted site sequence
MA0050.2	IRF1	17.317	0.881473027	182	202	−1	AGATGGA**GTCTTG**CTCTGTAG
MA0050.2	IRF1	12.077	0.821492265	177	197	−1	GA**GTCTTG**CTCTGTAGCCCAG
MA0050.2	IRF1	11.586	0.81587193	175	195	−1	**GTCTTG**CTCTGTAGCCCAGGC
MA0050.2	IRF1	11.23	0.811796901	190	210	−1	TTTTTTTGAGATGGA**GTCTTG**
MA0050.2	IRF1	10.835	0.80727545	186	206	−1	TTTGAGATGGA**GTCTTG**CTCT

The prediction of IRFs transcription factor BD in the *LP1* sequence using the online prediction software JASPAR (*http://jaspar.genereg.net/*). Only IRF1-binding sites among the IRFs family were predicted in the *LP1* region with higher scores. The predicted site sequences are given in their complementary chain.

deletion of unit-2 in the *IFNL2* promoter *LP1-1* sequence, and neither could be activated again by ATG10S overexpression. Instead, they showed lower levels of expression than by the ATG10 overexpression and in control groups. Therefore, we posited that the unit-2 oligonucleotide is necessary for ATG10S to promote *IFNL2* gene transcription. ATG10 had slightly opposing roles as ATG10S in both *LP1-1* and *LP1-1-ΔBD* promoter segments.

We performed comparative analyses of the five sequences of the predicted IRF1-binding domains (Table 1) and found that a common overlapping sequence (CAAGAC) (core motif, CM) existed in this unit-2 region (Table 1, Figures 2A and 3A). Next, we determined whether the CM was the locus for ATG10S binding on the *IFNL2* gene promoter. We similarly constructed plasmids of GFP and LUC reporter genes controlled by the CM-deleted *LP1-1* promoter (*ΔCM*) and detected their transcriptional activity under ATG10S overexpression. RT-PCR, western blotting, and the luciferase assay showed that both reporter genes were not expressed compared with *LP1-1* (Figure 3B–D). Consequently, the CM in *LP1-1* was found to be essential for the transcriptional activation of ATG10S on the *IFNL2* promoter. We simultaneously investigated which single nucleotide was responding to the binding role. Substituting individual nucleotides one-by-one in the CM (CAAGAC), 6 expression constructs of site-directed mutants labeled by GFP or LUC were produced and named *CM1[C > T], CM2[A > G], CM3[A > C], CM4 [G > T], CM5[A > G]*, and *CM6[C > T]* (Figure 3A). As shown in Figure 3B–D, the levels of GFP expression and activity of luciferase was not increased and were even decreased in *CM1 [C > T], CM3[A > C]*, and *CM6[C > T]* groups under ATG10S overexpression similar to the *ΔCM* group. The other three mutants still had transcription activity as the *LP1-1* group. Furthermore, as shown in Figure 3E, the DNA IP (DIP) assay showed that ATG10S but not ATG10 could bind to *LP1-1* DNA in HepG2 cells. When we deleted the CM or the three nucleotides were separately mutated in *CM1[C > T], CM3[A > C]*, and *CM6[C > T]* the combination of ATG10S with *LP1-1* disappeared. These results verified that CM1 (C), CM3 (A), and CM6 (C) within the CM (CAAGAC) of the *LP1-1* are crucial nucleotides for ATG10S binding on the *IFNL2* promoter. Any one mutation of the three nucleotides caused the loss of ATG10S function in *IFNL2* transcriptional activation.

ATG10S protein enters the nucleus by the classical nuclear transport system

Because ATG10S can activate the *IFNL2* promoter and suppress HCV replication [28,30], we determined how ATG10S entered the cell nucleus. We detected the subcellular distribution of ATG10S and compared it to that of ATG10 in both HepG2 cells and HCV-subreplicon cells using cell immunofluorescence (IF) experiments. The results showed that ATG10S distributed in both the cytoplasm and nucleus, but the nucleus had the most accumulation. The ATG10 protein did not dock in the nucleus and was only present in the peripheral cytoplasm of both cell lines (Figure 4A). Further, we assessed the subcellular localization of ATG10 and ATG10S by online prediction of the nuclear location signal (NLS) using cNLS Mapper software (http://nls-mapper.iab.keio.ac.jp/cgi-bin/NLS_Mapper_form.cgi) with the definition of the cutoff scores given in this work [26,31,32], in which the definition of the cutoff score specifies that a protein with a score equal to or higher than 3 can localize to both nucleus and cytoplasm, and a protein with a score below 3 can only localize to cytoplasm. The assessment indicated that ATG10 scores are less than 3, suggesting that the protein only localized in the cytoplasm; one of the ATG10S scores is 3.1, and the other three are below 3, which means ATG10S protein probably distributes in both cytoplasm and nucleus (Figure 4B). These predictions support this conclusion (Figure 4A). We then confirmed the ATG10S nucleus targeting by examining ATG10S conjugation with the nuclear transport protein KPNA1 and KPNB1 by co-immunoprecipitation (co-IP) experiments. The results showed that ATG10S and not ATG10 combined with endogenous KPNA1 and KPNB1 (Figure 4C), indicating that nuclear transport of ATG10S occurs via the classical nuclear transport pathway. Interestingly, the IRF1 protein was also conjugated with the complex (Figure 4C), suggesting that both IRF1 and ATG10S can translocate together into the nucleus, and HCV subreplicon did not affect ATG10S nucleus-docking. In response to the treatment of *KPNA1*-siRNA or *KPNB1*-siRNA, the phenomenon of ATG10S nucleus localization disappeared in the two experiments of nuclear-cytoplasmic separation and cell immunofluorescence (Figure 4D,E), which confirm that ATG10S nucleus transfer is indeed dependent on the classical nuclear transport pathway.

ATG10S activates IFNL2 *transcription via competition with IRF1 at the same core motif*

The results given above showed that the CM and CM1(C), CM3 (A), and CM6(C) are key loci and crucial nucleotides for ATG10S binding to the *IFNL2* promoter, which resulted from the prediction of the IRF1-binding site on the *IFNL2* promoter. The co-IP results showed that both IRF1 and ATG10S were both transferred by KPNA1 and KPNB1; however, the relationship between ATG10S and IRF1 in activating *IFNL2* transcription remains to be clarified. We investigated the interaction between

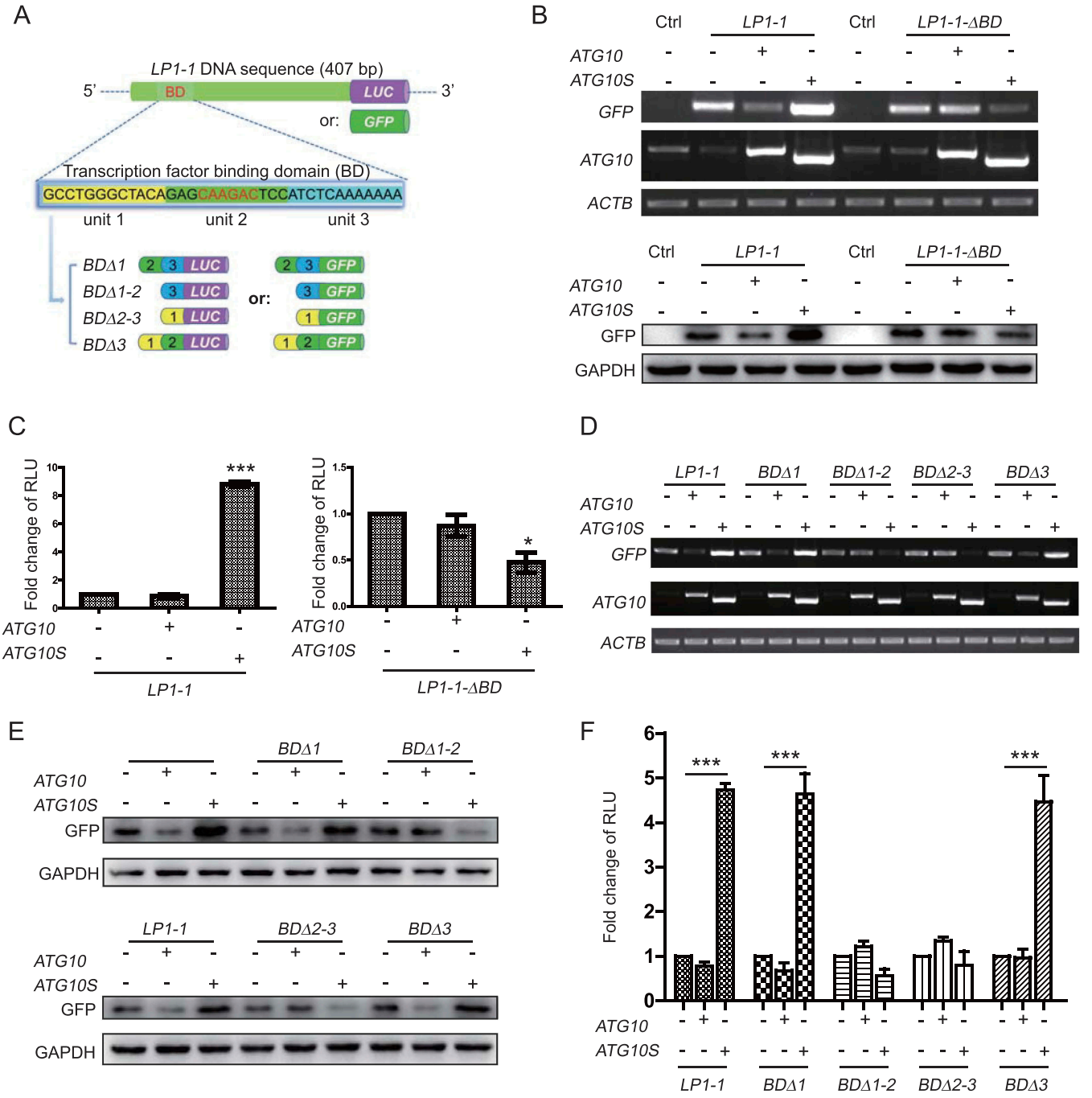

Figure 2. Transcription factor IRF1 Binding Domain (BD) is crucial for ATG10S promotion of *IFNL2* transcription. (A) Diagrams of *LP1-1*-GFP constructs with IRF1-BD deletion (*ΔBD*) and four pairs of oligonucleotide deletions in the BD. All of the mutants were cloned into pEGFP-ΔCMV-N1 (*GFP* as a reporter gene) and pGL3-basic (luciferase gene as a reporter gene) vectors. (B) GFP expression directed by *LP1-1* and *LP1-1-ΔBD* in HepG2 cells via co-transfected with *ATG10* or *ATG10S* mRNA were analyzed by RT-PCR (upper) and western blotting (bottom), Ctrl, non-transfection control. (C) The luciferase activity driven by *LP1-1* and *LP1-1-ΔBD* under co-transfected with *ATG10* or *ATG10S* mRNA were examined by luciferase assay. (D–F) ATG10/ATG10S-mediated activations of the oligonucleotide-deleted *LP1-1* mutants (*LP1-1-BDΔ1, LP1-1-BDΔ1-2, LP1-1-BDΔ2-3*, and *LP1-1-BDΔ3*) compared with *LP1-1* were detected using RT-PCR (D), western blotting (E), and luciferase assay (F). RLU, relative light unit. * indicates $P < 0.05$, *** $P < 0.001$. All of the statistics data are expressed as the mean ± SD (n = 3).

ATG10S and IRF1 using the luciferase activity analysis and qRT-PCR. When the endogenous *IRF1* transcript was knocked down by *IRF1* small interfering RNA (siRNA), the luciferase activity and *GFP* mRNA level significantly increased compared with the no *IRF1*-siRNA and Ctrl-siRNA groups under ATG10S overexpression with the *IFNL2 LP1-1* promoter; similarly, when downregulating *ATG10S*, the luciferase activity and *GFP* mRNA level was significantly higher in response to IRF1 overexpression than in the no *ATG10*-siRNA and Ctrl-siRNA groups (Figure 5A,B and F). Furthermore, we used a DNA IP experiment to confirm the direct competition relationship between ATG10S and IRF1 on *LP1-1*. When *IRF1*-siRNA downregulated IRF1, the amount of *LP1-1* DNA combined with ATG10S notably increased over both the no *IRF1*-siRNA and Ctrl-siRNA

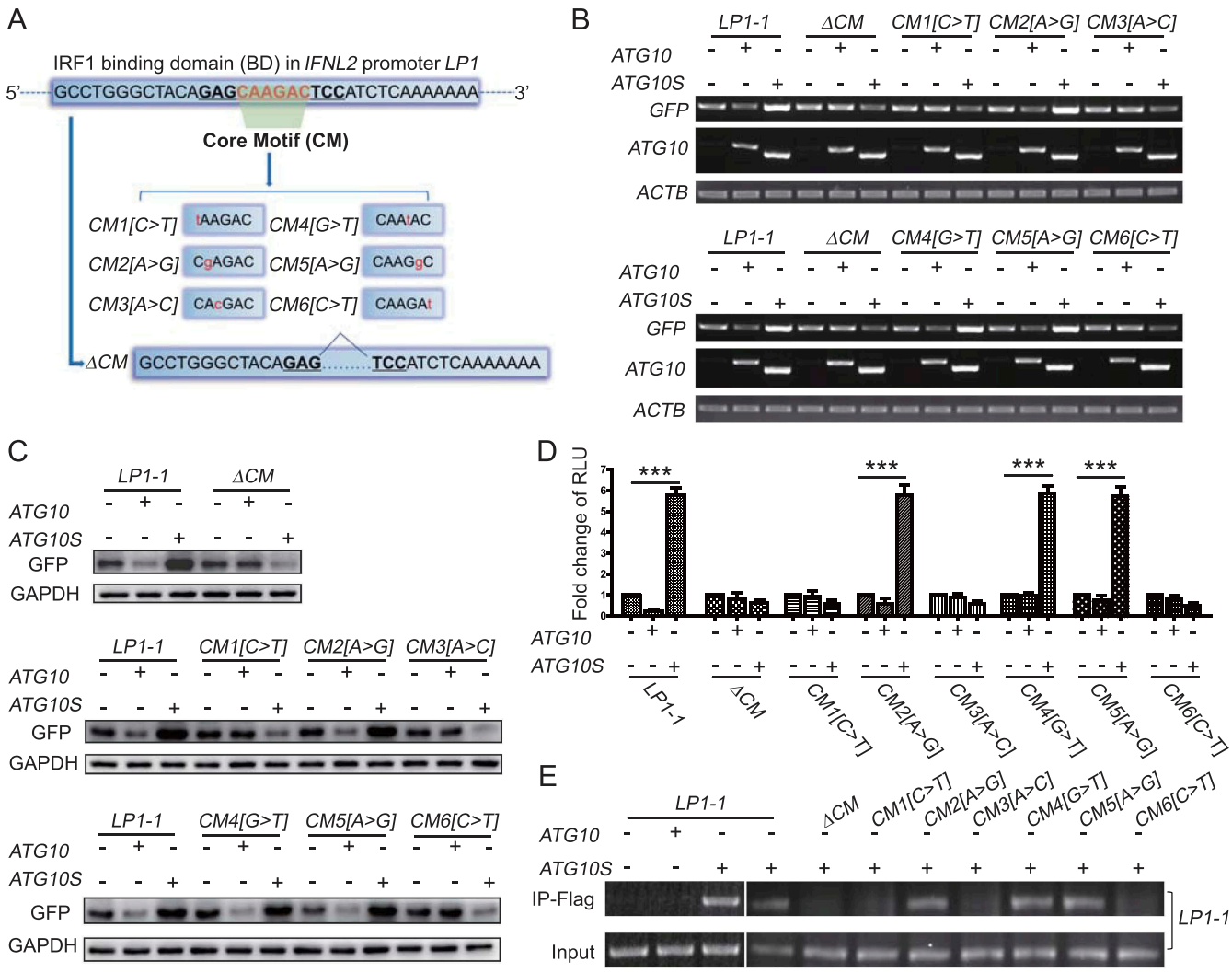

Figure 3. Crucial nucleotides of the *IFNL2 LP1-1* segment for ATG10S binding in the core motif (CM) of the IRF1-binding domain. (A) Diagram of CM deletion and six nucleotide-point mutations in the CM. These mutants were cloned into pEGFP-ΔCMV-N1 and pGL3-basic vectors. (B–D) Analysis of transcription activity driven by *LP1-1-ΔCM* or the point mutation constructs (*LP1-1-CM1[C > T], LP1-1-CM2[A > G], LP1-1-CM3[A > C], LP1-1-CM4[G > T], LP1-1-CM5[A > G]* or *LP1-1-CM6[C > T]* mutants) compared with *LP1-1* under ATG10 or ATG10S overexpression were detected by RT-PCR (B), western blotting (C), and luciferase assay (D). RLU, relative light unit. *** indicates $P < 0.001$. All of the data are expressed as the mean ± SD (n = 3). (E) DNA IP analysis of the interactions between ATG10S or ATG10 protein and *IFNL2* promoter *LP1-1* or *LP1-1* DNA mutation fragments (*LP1-1-CM1[C > T], LP1-1-CM2[A > G], LP1-1-CM3[A > C], LP1-1-CM4[G > T], LP1-1-CM5[A > G]* or *LP1-1-CM6 [C > T]*). These *IFNL2* promoter mutants were separately co-transfected with ATG10S or ATG10 into HepG2 cells. The cell lysates were immunoprecipitated with anti-FLAG antibody (FLAG-labeled with ATG10 and ATG10S) and followed PCR determination for these mutated *LP1-1* DNAs.

groups (Figure 5C). To determine if the competitive relationship exists on the same binding loci, we examined the BD and CM of the *IFNL2 LP1-1* segment using the same experiments and the same mutants. The results of the luciferase assay and RT-PCR showed that the effects of IRF1 on *IFNL2* transcription significantly reduced in the *LP1-1* mutants of the BD-deleted, BD-unit2-deleted, CM-deleted, *CM3[A > C]*, and *CM4[G > T]* groups, but were moderately raised in the *CM6[C > T]* group compared with the wild-type *LP1-1* group (Figure 5D and E). These results suggested that the CM3 (A) and CM4 (G) are necessary nucleotides for IRF1 binding on the *IFNL2 LP1-1* promoter. The *CM6[C > T]* mutation enhanced *IFNL2* transcription, but *CM1[C > T]* did not affect IRF1. Thus, CM3 (A) is a common key nucleotide for both IRF1 and ATG10S binding to the same promoter, CM4 (G) is a specific nucleotide for IRF1 binding, and CM6 (C) has opposite effects on IRF1 and ATG10S. However, CM deletion caused a decrease of both IRF1 and ATG10S activity (Figures 5D, E and 3B–E), and IRF1 or ATG10S downregulation led to the increase of ATG10S or IRF1 activity, respectively (Figure 5A and B). Therefore, we infer that ATG10S can activate *IFNL2* transcription via competition with IRF1 at the same binding site (the core motif), but the individual nucleotides for ATG10S and IRF1 binding loci are different.

ATG10 inhibits the GFP expression

We also observed an intriguing phenomenon that overexpression of ATG10 moderately inhibited GFP expression. We infer that ATG10 overexpression can promote autophagosome formation, which contributes to the degradation of excess

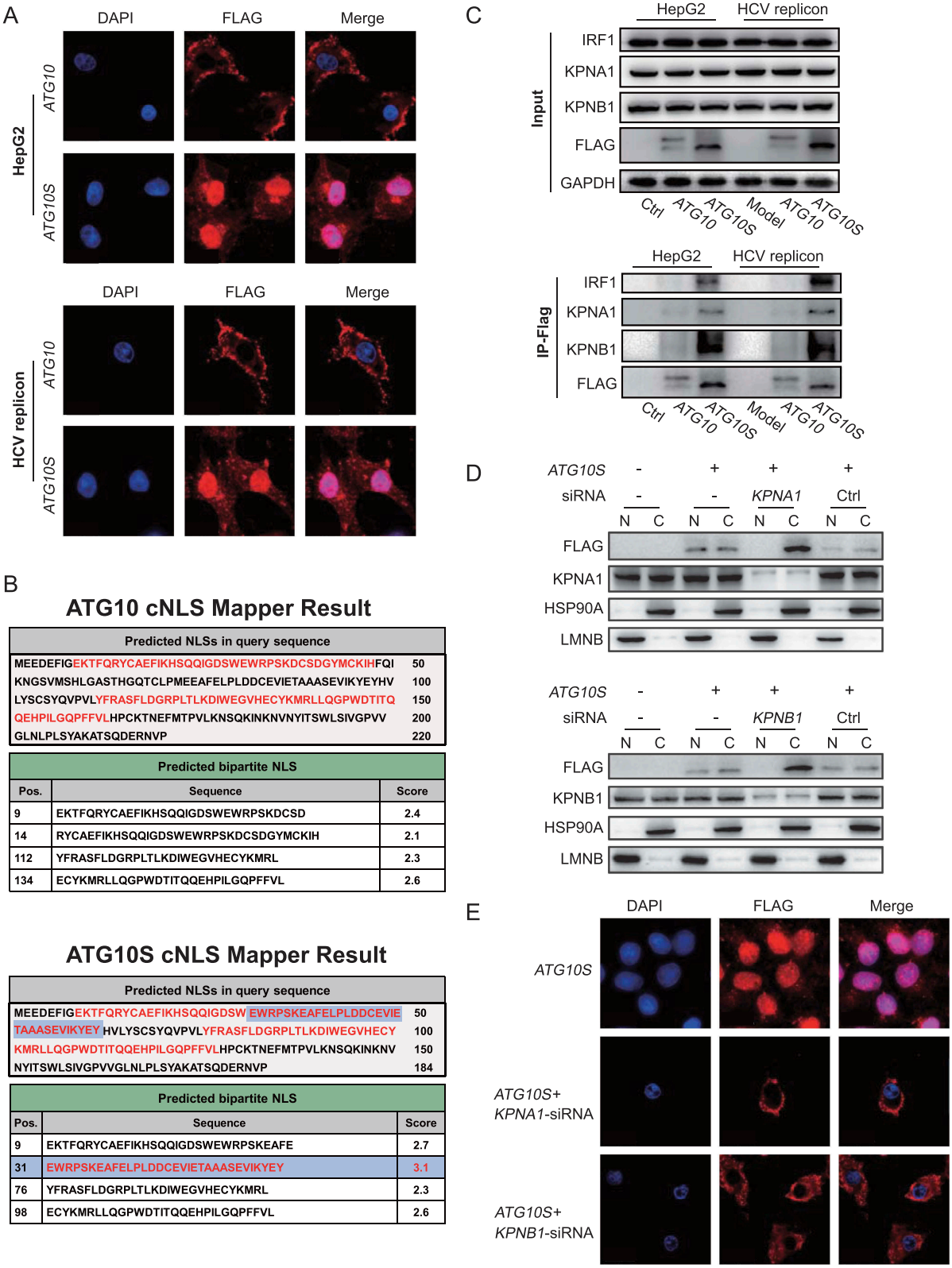

B

ATG10 cNLS Mapper Result

Predicted NLSs in query sequence	
MEEDEFIGEKTFQRYCAEFIKHSQQIGDSWEWRPSKDCSDGYMCKIHFQI	50
KNGSVMSHLGASTHGQTCLPMEEAFELPLDDCEVIETAAASEVIKYEYHV	100
LYSCSYQVPVLYFRASFLDGRPLTLKDIWEGVHECYKMRLLQGPWDTITQ	150
QEHPILGQPFFVLHPCKTNEFMTPVLKNSQKINKNVNYITSWLSIVGPVV	200
GLNLPLSYAKATSQDERNVP	220

Predicted bipartite NLS		
Pos.	Sequence	Score
9	EKTFQRYCAEFIKHSQQIGDSWEWRPSKDCSD	2.4
14	RYCAEFIKHSQQIGDSWEWRPSKDCSDGYMCKIH	2.1
112	YFRASFLDGRPLTLKDIWEGVHECYKMRL	2.3
134	ECYKMRLLQGPWDTITQQEHPILGQPFFVL	2.6

ATG10S cNLS Mapper Result

Predicted NLSs in query sequence	
MEEDEFIGEKTFQRYCAEFIKHSQQIGDSWEWRPSKEAFELPLDDCEVIE	50
TAAASEVIKYEYHVLYSCSYQVPVLYFRASFLDGRPLTLKDIWEGVHECY	100
KMRLLQGPWDTITQQEHPILGQPFFVLHPCKTNEFMTPVLKNSQKINKNV	150
NYITSWLSIVGPVVGLNLPLSYAKATSQDERNVP	184

Predicted bipartite NLS		
Pos.	Sequence	Score
9	EKTFQRYCAEFIKHSQQIGDSWEWRPSKEAFE	2.7
31	EWRPSKEAFELPLDDCEVIETAAASEVIKYEY	3.1
76	YFRASFLDGRPLTLKDIWEGVHECYKMRL	2.3
98	ECYKMRLLQGPWDTITQQEHPILGQPFFVL	2.6

Figure 4. ATG10S can be transported into the nucleus, and bind on the *IFNL2*-core motif as a transcription factor. (A) Representative immunocytochemical images of ATG10 and ATG10S distribution in HepG2 cells and HCV replicon cells via using anti-FLAG antibody (FLAG labeled to ATG10 or ATG10S). Scale bars: 15 μm. (B) Prediction of NLS in ATG10 and ATG10S using online prediction software (http://nls-mapper.iab.keio.ac.jp/cgi-bin/NLS_Mapper_form.cgi). Based on the software, a score of a protein is greater than 3, indicating that the protein can distribute in both the nucleus and cytoplasm; a protein score less than 3 suggests the protein only localizes in the cytoplasm. (C) Interactions among ATG10S, KPNA1, KPNB1, and IRF1 in HepG2 and HCV subreplicon cells by co-IP. Cells transfected with the *ATG10S* or *ATG10* constructs, the cell lysates were immunoprecipitated with anti-FLAG antibody and the proteins were detected by immunoblot assay. (D, E) Subcellular localization of ATG10S protein was determined by nuclear-cytoplasmic fractionation (D) and cell-IF (E) under KPNA1 or KPNB1 knockdown using *KPNA1*-siRNA or *KPNB1*-siRNA, respectively.

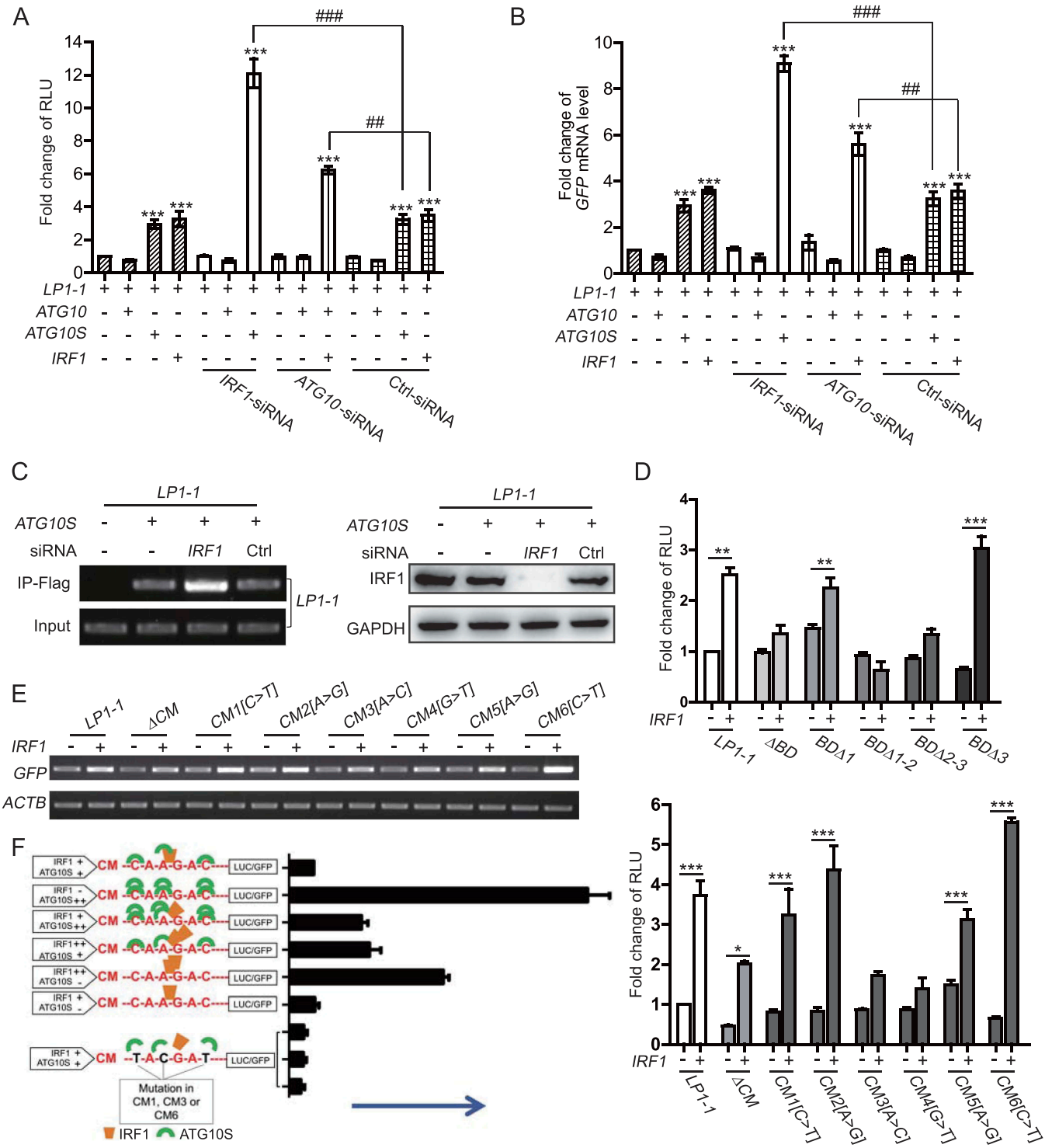

Figure 5. ATG10S activates IFNL2 transcription via competition with IRF1 at the same core motif. (A, B) Activity of *IFNL2* promoter *LP1-1* was competitively induced by ATG10S and IRF1 in Luciferase activity assay (A) and qRT-PCR (B) using gene upregulation and downregulation of *ATG10S* and *IRF1* genes. (C) DNA IP analysis of ATG10S binding to *LP1-1* DNA with *IRF1*-siRNA compared with no *IRF1*-siRNA and Ctrl-siRNA groups in HepG2 cells. The cell lysates were immunoprecipitated with anti-FLAG antibody and *LP1-1* DNA were detected by RT-PCR (left panel), IRF1 downregulation was confirmed by western blotting (right panel). (D) Luciferase activity analysis of *LP1-1* sequential deletions (*LP1-1-ΔBD, LP1-1-BDΔ1, LP1-1-BDΔ1-2, LP1-1-BDΔ2-3*, and *LP1-1-BDΔ3*) groups compare to *LP1-1* group (upper panel), and of the CM deletion and six-point mutants (*LP1-1-ΔCM, LP1-1-CM1[C > T], LP1-1-CM2[A > G], LP1-1-CM3[A > C], LP1-1-CM4[G > T], LP1-1-CM5[A > G]*, and *LP1-1-CM6 [C > T]*) groups compare to *LP1-1* group (bottom panel) under IRF1 overexpression. (E) *GFP* transcription directed by *LP1-1, LP1-1-ΔCM, LP1-1-CM1[C > T], LP1-1-CM2 [A > G], LP1-1-CM3[A > C], LP1-1-CM4[G > T], LP1-1-CM5[A > G]*, and *LP1-1-CM6[C > T]* mutants under IRF1 overexpression were analyzed by RT-PCR. (F) A model of competitive binding loci for IRF1 and ATG10S on the CM and their corresponding inductive activity. + indicates endogenous IRF1 or ATG10S expression, ++ indicates IRF1 or ATG10S overexpression, – indicates endogenous IRF1 or ATG10S knockdown. * indicates $P < 0.05$, ** and ## indicates $P < 0.01$, *** and ### indicates $P < 0.001$. All data are expressed as the mean ± SD (n = 3).

intracellular protein via autophagic digestion, so the presence of ATG10 overexpression degraded more GFP than in the control group. Two co-IP and DNA IP experiments demonstrated this hypothesis. Both results show that when using immunoprecipitation with anti-LC3B and anti-SQSTM1/p62 antibodies, massively more GFP protein and *GFP* mRNA combined with LC3B and SQSTM1 proteins appeared under ATG10 overexpression than in the control group (Figure S1), meaning that more GFP products than those in the control group were transferred into autophagosome and degraded.

Discussion

Our recent studies showed that the two isoforms of ATG10 and ATG10S have distinct roles in HCV subgenome replication and autophagy flux. ATG10S activates expression of *IFNL2* and also promotes the formation of autolysosomes with the help of IFNL2, leading to degradation of HCV subgenome and HCV virion by driving autophagy flux [28,30]. Here, we confirmed this action of ATG10S suppression on HCV subreplicon and full virion again (Figure S2). We believe that the anti-HCV activity may be correlated with IFNL2 expression activated by ATG10S. We found that ATG10S translocated into the nucleus, which raised the possibility that ATG10S might act as a latent transcription factor [30]. The current study is a continuation of our previous studies and explores the molecular mechanism of ATG10S promoting IFNL2 expression. We found that ATG10S could bind to the *IFNL2* promoter *LP1-1* segment, which was about 1 kb upstream sequence of the initial codon by a series of sequential promoter deletion and DNA IP assays, which is in accordance with the report from Hahn's group [33]. The canonical longer isoform ATG10 did not have similar roles as ATG10S. Prediction of a protein's subcellular localization using software is a useful tool for an initial study of a new protein function [34,35]. We utilized cNLS Mapper software online predicted the characteristic of ATG10S protein in subcellular localization. Prediction of the NLS showed that the ATG10S protein has the potential to localize in both the cytoplasm and nucleus. ATG10S is translocated to the nucleus by KPNA1 and KPNB1 in a ternary complex, as confirmed by co-IP and IF. This study also revealed that ATG10S could recognize a specific motif and nucleotides in the *IFNL2* promoter sequence, indicating that it has characteristics of a transcription factor and acts as a transcription factor to promote *IFNL2* transcription.

Another significant finding was that the binding site of ATG10S was the same BD for the IRF1 transcription factor, indicating that ATG10S and IRF1 compete for binding at the same locus. The relationship between ATG10S and IRF1 was identified by siRNA and showed a negative correlation; knockdown of endogenous IRF1 significantly increased the activity of ATG10S toward *IFNL2* gene transcription. The crucial nucleotides were detected for ATG10S and IRF1 binding by nucleotide mutations, which showed differential nucleotides, but CM3 (A) was common for binding of both. ATG10S and IRF1 share a CM (CAAGAC) but have their specific nucleotide pattern (CM1 [C], CM3 [A], and CM6 [C]) for ATG10S, the CM3 (A) and CM4 (G) for IRF1 for binding to the *IFNL2* promoter. Thus, we inferred that there is probably crosstalk and interaction between ATG10S and IRF1 proteins. Although they act on different nucleotides besides sharing CM3 (A), the special hindrance disturbs their simultaneous binding to the CM (Figure 5F), which may limit their synergistic effects on IFNL2 activation. This result may illustrate why ATG10S has stronger activity in promoting *IFNL2* transcription after IRF1 downregulation.

Previous studies have shown that the *IFNL1* gene is regulated by IRF3 and IRF7, similar to the *IFNB1* gene, whereas *IFNL2* and *IFNL3* gene expression is mainly controlled by IRF7, which is similar to transcription of the *IFNA2* gene [10]. However, in accordance with previous research results, we found that the transcriptional regulation of *IFNL* genes may be dependent on cell- or stimulus-specific induction patterns [10,36–38]. To date, the views on the interaction between IRFs and IFNLs are complex and inconclusive. One study showed that *IFNL1* gene expression requires IRFs binding to spatially separated elements in distal regions of the promoter [36], whereas another report demonstrated that proximal regions (1 kb) of the promoter are involved in HCV–induced production of IFNL [33]. In this study, we found that overexpression of IRF1 can also promote IFNL2 overexpression, and the action site is located within 1 kb upstream sequence from *IFNL2* initial codon. An interesting phenomenon is that after CM3 or CM4 mutation in the CM of the *IFNL2* promoter *LP1-1* sequence, the activity of IRF1 in promoting IFNL2 expression was clearly lower than that on wildtype *LP1-1*, but still moderately displayed compared with the control group (Figure 5D and E). Therefore, we postulate that IRF1 regulatory roles on IFNL2 activation differ from those of ATG10S, even if they act at the same CM sequence in *LP1-1*. Accordingly, the regulatory mechanism of *IFNL2* gene expression may be related to the complex regulation of multiple transcription factors, including other regulatory elements and other binding sites on the *IFNL2* promoter. Our results demonstrated that ATG10S functions similarly to the *IFNL2* transcription factor, indicating a new innate immune regulation pathway. According to our previous studies [28,30], this study also provides evidence of communication between autophagy and the innate immune system.

IFNs represent the first line of defense against viral pathogens and act directly on viral replication and indirectly through the activation of host immune response genes [39]. Previous studies have reported that IFNL resists HCV by using both HCV replicon and cell culture infectious virus model systems in hepatocellular carcinoma cells, and other viruses, including HIV, HBV, and influenza A virus are sensitive to the antiviral effects of IFNL [3,4]. These results confirm that IFNL proteins are potent antiviral cytokines. However, some studies have found that the expression of IFNL is enhanced in patients with chronic HCV [33], indicating that endogenous IFNL produced by the innate immune response is insufficient to clear HCV virus, or that HCV can effectively evade the antiviral effects of IFNL. In recent years, our group found that ATG10S can significantly promote the high expression of type III IFN and may act as a transcription factor to regulate *IFNL2* gene expression [28,30]. Additional studies are needed to determine whether ATG10S may be a novel target for the screening of antiviral drugs. The results of this study clarified the molecular mechanism by which ATG10S inhibits HCV replication. ATG10S, as a restrictive host factor, promotes the overexpression of type III IFN, while whether ATG10S has a similar effect on other viruses needs to be

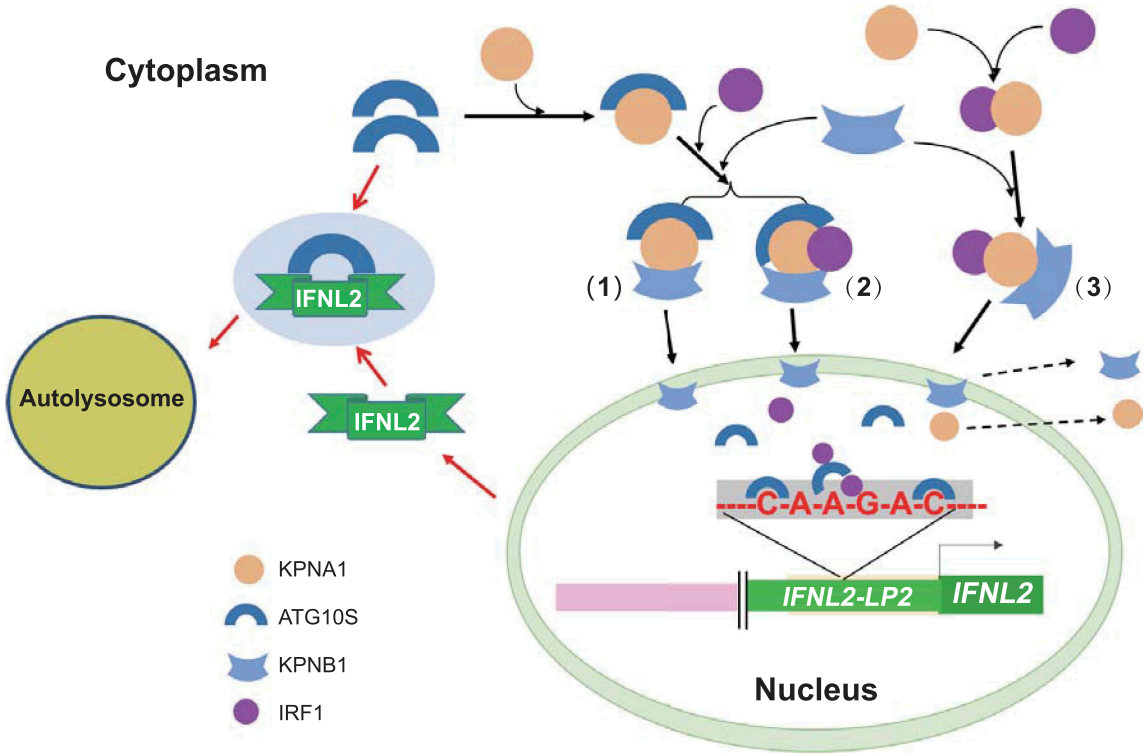

Figure 6. Overview of ATG10S function as both an autophagy activator and a novel transcription factor in HepG2 cells. (1) ATG10S is transferred into the nucleus by KPNA1 and KPNB1 when IRF1 is downregulated. (2) ATG10S is transferred into the nucleus together with IRF1 by KPNA1 and KPNB1. (3) IRF1 is transferred into the nucleus by KPNA1 and KPNB1 in the presence of little or no ATG10S expression. The red arrows show that ATG10S can cooperate with IFNL2 in promoting autophagy flux in the cytoplasm, as reported in our previous studies [28,30] The black arrows show the transport of ATG10S into the nucleus carrying by KPNA1 and KPNB1 proteins and binding to the CM of the *IFNL2* promoter at different sites from IRF1, but only one nucleotide is shared with IRF1 at *IFNL2*: CM3-Adenine.

further explored. Moreover, due to its high homology to IFNL family members, it also needs to be determined if ATG10S can activate the expression of other members of the type III IFN family by a similar mechanism of promoting IFNL2 expression.

In summary, our findings suggest that ATG10S is transported into the nucleus by the classical nuclear transport system, where it competes with IRF1 for binding to the CM to promote transcription of IFNL2 (Figure 6).

Materials and methods

Antibodies and reagents

Anti-FLAG antibody for co-IP, IF, and DNA IP assay was obtained from Abcam (ab1257). For co-immunoprecipitation (co-IP) and DNA IP assay, anti-SQSTM1/p62 (PM045) and anti-LC3B (PM036) were obtained from MBL (PM045). For immunoblot analysis, anti-GFP (M048-3), anti-LC3B (M186-3), and anti-SQSTM1/p62 (PM045) were purchased from MBL International Corporation; anti–IFNL2 (ab38570), anti–IRF1 (ab186384), anti-KPNB1/importin β (ab45938), anti-HSP90A/Hsp90 (ab13495), anti-NS5B (ab122972), and anti-CORE (ab2740) were obtained from Abcam; anti-KPNA1/importin α (14372) was obtained from Cell Signaling Technology; anti-LMNB/lamin B (sc-6216) was purchased from Santa Cruz Biotechnology; and anti-GAPDH (TA-08) and horseradish peroxidase-conjugated goat anti-rabbit (ZB-2301), goat anti-mouse (ZB-2305), and rabbit anti-goat (ZB-2306) IgG were purchased from Zsgb Bio. For IF, FITC-labeled goat anti-mouse IgG (ZF-0312), TRITC-labeled goat anti-rabbit IgG (ZF-0316), and TRITC-labeled rabbit anti-goat IgG (ZF-0317) secondary antibodies, and mounting medium with DAPI (ZLI-9557) were purchased from Zsgb Bio. For co-IP experiments, mouse IgG (A7028) and rabbit IgG (A7016) were purchased from Beyotime Biotechnology, and protein A/G plus agarose (sc-2003) was obtained from Santa Cruz Biotechnology. Lipofectamine 2000 Reagent (1815626) was purchased from Invitrogen. Protein extraction reagent RIPA lysis buffer (C1053), protease inhibitor (cocktail, 50x, P1261-1), and non-denaturing lysis buffer (C1050) were purchased from Applygen Technologies, Inc.

Cell lines and HCV models

HepG2 cells were obtained from the National Infrastructure of Cell Line Resource. HCV subgenomic replicon cell model was constructed in accordance with our previous work using prGC3N and p5BR (constructed in our previous study [40]) co-transfected into HepG2 cells [28,40]. The HCV subgenomic replicon sequence was cloned from HCV 1b genomic sequence; prGC3N expresses antisense HCV 5′ UTR-core sequence and sense 3′ UTR, which acts as the HCV RNA subgenomic template; and p5BR expresses HCV RNA-dependent RNA polymerase NS5B. HCV virion infection cells were performed as previously described [28]. Briefly, Huh7.5 cells (provided by Dr. Zonggen Peng) were separately transfected with *ATG10* and *ATG10S* constructs, after 6 h culture, infected with HCV virions (HCV 2a, J6/JFH/JC, 45 IU/cell) (provided by Dr. Zonggen Peng) for 72 h and

collected for succeeding experiments. Cells were cultured in MEM (Gibco, 8119340) supplemented with 10% fetal bovine serum (Gibco, 2025790) at 37°C in a 5% CO_2 incubator.

Plasmid construction

ATG10 and ATG10S with FLAG-tagged at their N-terminals constructs were designed as previously described [28,30]. *IFNL2* promoter of 2.1 kb sequence was cloned using PCR with two pairs of primers and inserted into the pEGFP-ΔCMV-N1 vector in which the CMV promoter sequence was deleted and replaced by the designed segments of the *IFNL2* promoter in pEGFP-N1 (Solarbio, P6460). The 2 primer pairs (5′-3′) were as follows: *LP2* (F-GCCCCAC AGCCAGCTTTGAGATT, R-TCCTGATCTCTGGTCTTT GTC); *LP1* (F-CGTGGTGGTGCATGCCTATAGTC, R-TC CTGATCTCTGGTCTTTGTC). The fragment deletion mutants of *LP1-1, LP1-2*, and *LP1-3* were cloned into the pEGFP-ΔCMV-N1 vector (Figure 1E). A series of truncated *LP1-1* mutants were constructed based on 3 units of the predicted IRF1 transcription factor BD. The 3 units were deleted from the 5′-terminal or 3′-terminal sequentially and inserted into the pEGFP-ΔCMV-N1 vector and pGL3.0-basic vector (Promega, E1751), forming four truncated mutants: *BDΔ1, BDΔ1-2, BDΔ2-3*, and *BDΔ3* (Figure 2A). Point mutation constructs were generated using the QuikChange Site-Directed Mutagenesis Kit (Beyotime Biotechnology, D0206) and ligated into the pEGFP-ΔCMV-N1 and pGL3.0-basic vectors (Figure 3A). Site-directed mutagenesis was done as follows: *CM1[C > T]* (CAAGAC changed to tAAGAC); *CM2 [A > G]* (CAAGAC changed to CgAGAC); *CM3[A > C]* (CAAGAC changed to CAcGAC); *CM4[G > T]* (CAAGAC changed to CAAtAC); *CM5[A > G]* (CAAGAC changed to CAAGgC); *CM6[C > T]* (CAAGAC changed to CAAGAt).

Transfection and luciferase assay

Cells were transfected with 1 μg *GFP* reporter plasmid driven by the *IFNL2* promoter and 100 ng 5′-capped mRNAs of *ATG10, ATG10S*, or *IRF1* by using Lipofectamine 2000 reagent (Invitrogen, 1815626) according to the manufacturer's instructions. Then the cells were collected after 30 h of culture for subsequent experiments. For the luciferase assay, cells were transfected with 1 μg plasmids of luciferase reporter driven by the *IFNL2* promoter and 10 ng pRL-SV40-N plasmid (Beyotime Biotechnology, D2762), and co-transfected with *ATG10, ATG10S*, or *IRF1* 5′ capped-mRNAs. After 30 h, cells were harvested and lysed in 250 μL lysis buffer (Beyotime Biotechnology, RG027-1) for *firefly* luciferase and *Renilla* luciferase activities assay by using the Dual-Luciferase Reporter Gene Assay Kit (Beyotime Biotechnology, RG027) according to the manufacturer's instructions. Data are expressed as the mean relative luciferase activity plus SD for one representative experiment conducted in triplicate of at least 3 independent experiments.

DNA IP assay

Briefly, we transfected HepG2 cells separately with FLAG-tagged *ATG10* and *ATG10S* mRNA, and co-transfected with *IFNL2* promoter constructs. We harvested cells and added 1% formaldehyde. The culture was incubated at 37°C for 10 min to allow the cross-linking of proteins and DNA. Following 3 times of wash with cold 1 mM PMSF (Beyotime Biotechnology, ST506), the cells were resuspended using SDS lysis buffer containing 1% SDS and 1 mM PMSF and lysed by sonication. After centrifugation, the supernatant was collected, and the DNA in the supernatant was immunoprecipitated with anti-FLAG, anti-LC3B, and anti-SQSTM1/p62 antibodies. Immunoprecipitated DNA was measured by RT-PCR using *LP1-1* or *GFP* specific primers (synthesized by Sangon Biotech). The primer sequences were as follows: *LP1-1* (forward primer, 5′-CGTGGTGGTGCAT GCCTATA-3′ and reverse primer, 5′-TAACTGCAACCTCC ACCTCC-3′); *GFP* (forward primer, 5′-ACGGCGTGCAGTG CTT-3′, reverse primer, 5′-TGGGTGCTCAGGTAGTGG-3′).

PCR assay

Total RNA was extracted using Trizol Reagent (Invitrogen, 15596–026), and first-strand complementary DNA (cDNA) was synthesized from 1.0 μg total RNA using M-MLV reverse transcriptase (Promega, M1708) according to the manufacturer's instructions. PCR was performed with primer pairs (synthesized by Sangon Biotech) of related genes, and *ACTB/β-ACTIN* expression served as the reference gene for all of the reactions. The primer sequences (5′-3′) for RT-PCR are as follows: *ATG10* or *ATG10S* (F-ATGGAAGAAGATGAGTTCATTGG, R-TTA AGGGACATTTCGTTCATCCTGAG); *GFP* (F-ACGGCGT GCAGTGCTT, R-TGGGTGCTCAGGTAGTGG); *ACTB* (F-AGGGAAAT CGTGGGTGACATCAAA, R-ACTCATC GTACTCCTGCTTGCTGA). The primer sequences for quantitative real-time PCR (qRT-PCR) (5′-3′) are as follows: *IFNL2* (F-AATTGTGTTGCCAGTGGGGA, R- GCGACTGGGTGGC AATAAAT); *GFP* (F-AGATCCGCCACAACATCGAG, R-GTCCATGCCGAGAGTGATCC); *ACTB* (F-CACCATTGGCA ATG AGCGGTTC, R-AGGTCTTTGCGGATGTCCACGT).

Co-immunoprecipitation (Co-IP) and cell immunofluorescence

As previously described [30], for co-IP experiments, HepG2 and HCV subgenomic replicon cells transiently transfected with *ATG10* or *ATG10S* plasmids for 30 h. Then the cells were lysed with non-denaturing lysis buffer containing protease inhibitor cocktail (Applygen Technologies, P1261-1), and the lysate was incubated with anti-FLAG, anti-LC3B, and anti-SQSTM1 antibodies. Protein-antibody immune complexes were washed with lysis buffer, dissolved in SDS loading buffer, and subsequently subjected to immunoblot analysis. For cell immunofluorescence, the cells were seeded on coverslips and transiently transfected with *ATG10* or *ATG10S* plasmids for 30 h. Cells nuclei were stained with DAPI (Zsgb Bio, ZLI-9557), and TRITC-anti-FLAG antibodies were used to visualize the subcellular location of ATG10 or ATG10S.

Nuclei–cytoplasm fractionation experiment

FLAG-tagged *ATG10S* mRNA co-transfected with *KPNA1*-siRNA (Santa Cruz Biotechnology, sc-41277) or *KPNB1*-siRNA (Santa Cruz Biotechnology, sc-35736) into HepG2 cells, and the cells were collected for the subsequent experiments after 36 h culture. Nuclei and cytoplasm fractionation were conducted using the NE-PER Nuclear and Cytoplasmic Extraction Reagents kit (Thermo Fisher Scientific, 78835) according to the manufacturer's protocol. Western blot analysis was performed to detect ATG10S in both parts of nuclei and cytoplasm using the anti-FLAG antibody. LMNB and HSP90A served as the nuclear marker and cytoplasmic marker, respectively.

Overexpression and siRNA-mediated knockdown of IRF1

First, *IRF1* sequence was cloned into pGEM-T vector (Promega, A1380). To assess the action of IRF1 action on transcription of *IFNL2*, 5′-capped mRNAs of *IRF1* were synthesized *in vitro* using a capped mRNA kit (Ambion, AM1348) with pGEM-T-*IRF1* as templates. Each 100 ng 5′-capped mRNA or mock plasmid and plasmids of the reporter gene guided by the *IFNL2* promoter were co-transfected into HepG2 cells for each well. Then the cells were collected after 30 h for subsequent experiments. To knockdown the expression of *IRF1, IRF1*-siRNA was obtained from Santa Cruz Biotechnology, and siRNA transfection was performed as described in the user manual (sc-35706).

SiRNA-mediated knockdown of ATG10S

ATG10-siRNA was obtained from Santa Cruz Biotechnology, and siRNA transfection was performed as described in the user manual (sc-72576). *ATG10*-siRNA is a pool of three different siRNA duplexes; their sequences are as follows: sc-72576A, 5′GGAGACCUUUAACUCUGAAtt3′ (sense) and 5′UUCAGAGUUAAAGGUCUCCtt3′ (antisense); sc-72576B, 5′GUACUUCAUCCCUGCAAGAtt3′ (sense) and 5′UCUUG CAGGGAUGAAGUACtt3′ (antisense); sc-72576C: 5′GAAUC UACCUCUGAGUUAUtt3′ (sense) and 5′AUAACUC AGAGGUAGAUUCtt3′ (antisense). Because the *ATG10*-siRNA can cause downregulation of both ATG10 and ATG10S, in order to prevent ATG10 deficiency from skewing ATG10S result, *ATG10*-siRNA plus ATG10 (long one) overexpression was used in this test. (Figure 5A and B).

Statistical analysis

Data analysis was performed using GraphPad Prism 7 software. Statistical comparisons were made using analysis of variance (ANOVA) and Student's t test. Data are expressed as the mean ± SD from three independent experiments, and P-values less than 0.05 were considered to be statistically significant.

Acknowledgments

We thank Dr. Zonggen Peng and Jianrui Li for providing Huh7.5 cell line and HCV virion and the experimental condition. LetPub (www.letpub.com) for the linguistic assistance of this manuscript.

Disclosure statement

No potential conflict of interest was reported by the authors.

Funding

This work was supported by The National Natural Science Foundation of China [No. 81373453], the Chinese National Key Technology R&D Program [2015BAK45B01], and Foundation for Innovative Research Groups of the National Natural Science Foundation of China [81621064].

References

[1] Zhu M, Fang T, Li S, et al. Bipartite nuclear localization signal controls nuclear import and DNA-binding activity of IFN regulatory factor 3. J Immunol. 2015;195(1):289–297. PubMed PMID: 25994966.
[2] Li M, Liu X, Zhou Y, et al. Interferon-lambdas: the modulators of antivirus, antitumor, and immune responses. J Leukoc Biol. 2009;86(1):23–32. PubMed PMID: 19304895.
[3] Zhu H, Butera M, Nelson DR, et al. Novel type I interferon IL-28A suppresses hepatitis C viral RNA replication. Virol J. 2005;2:80. PubMed PMID: 16146571.
[4] Robek MD, Boyd BS, Chisari FV. Lambda interferon inhibits hepatitis B and C virus replication. J Virol. 2005;79 (6):3851–3854. PubMed PMID: 15731279.
[5] Zhang L, Jilg N, Shao RX, et al. IL28B inhibits hepatitis C virus replication through the JAK-STAT pathway. J Hepatol. 2011;55 (2):289–298. PubMed PMID: 21147189.
[6] Lund JM, Alexopoulou L, Sato A, et al. Recognition of single-stranded RNA viruses by toll-like receptor 7. Proc Natl Acad Sci U S A. 2004;101(15):5598–5603. PubMed PMID: 15034168.
[7] Pei RJ, Chen XW, Lu MJ. Control of hepatitis B virus replication by interferons and toll-like receptor signaling pathways. World J Gastroenterol. 2014;20(33):11618–11629. PubMed PMID: 25206268.
[8] Gad HH, Dellgren C, Hamming OJ, et al. Interferon-lambda is functionally an interferon but structurally related to the interleukin-10 family. J Biol Chem. 2009;284(31):20869–20875. PubMed PMID: 19457860.
[9] Lee S, Baldridge MT. Interferon-lambda: a potent regulator of intestinal viral infections. Front Immunol. 2017;8:749. PubMed PMID: 28713375.
[10] Osterlund PI, Pietila TE, Veckman V, et al. IFN regulatory factor family members differentially regulate the expression of type III IFN (IFN-lambda) genes. J Immunol. 2007;179(6):3434–3442. PubMed PMID: 17785777.
[11] Ikushima H, Negishi H, Taniguchi T. The IRF family transcription factors at the interface of innate and adaptive immune responses. Cold Spring Harb Symp Quant Biol. 2013;78:105–116. PubMed PMID: 24092468.
[12] Barnes B, Lubyova B, Pitha PM. On the role of IRF in host defense. J Interferon Cytokine Res. 2002;22(1):59–71. PubMed PMID: 11846976.
[13] Matta B, Song S, Li D, et al. Interferon regulatory factor signaling in autoimmune disease. Cytokine. 2017;98:15–26. PubMed PMID: 28283223.
[14] Fujii Y, Shimizu T, Kusumoto M, et al. Crystal structure of an IRF-DNA complex reveals novel DNA recognition and cooperative binding to a tandem repeat of core sequences. Embo J. 1999;18(18):5028–5041. PubMed PMID: 10487755.
[15] Escalante CR, Yie J, Thanos D, et al. Structure of IRF-1 with bound DNA reveals determinants of interferon regulation. Nature. 1998;391(6662):103–106. PubMed PMID: 9422515.
[16] Yanai H, Negishi H, Taniguchi T. The IRF family of transcription factors: inception, impact and implications in oncogenesis. Oncoimmunology. 2012;1(8):1376–1386. PubMed PMID: 23243601.

[17] Romeo G, Fiorucci G, Chiantore MV, et al. IRF-1 as a negative regulator of cell proliferation. J Interferon Cytokine Res. 2002;22 (1):39–47. PubMed PMID: 11846974.
[18] Sun L, Liu S, Chen ZJ. SnapShot: pathways of antiviral innate immunity. Cell. 2010;140(3):436- e2. PubMed PMID: 20144765.
[19] Honda K, Taniguchi T. IRFs: master regulators of signalling by toll-like receptors and cytosolic pattern-recognition receptors. Nat Rev Immunol. 2006;6(9):644–658. PubMed PMID: 16932750.
[20] Tamura T, Yanai H, Savitsky D, et al. The IRF family transcription factors in immunity and oncogenesis. Annu Rev Immunol. 2008;26:535–584. PubMed PMID: 18303999.
[21] Shultz DB, Rani MR, Fuller JD, et al. Roles of IKK-beta, IRF1, and p65 in the activation of chemokine genes by interferon-gamma. J Interferon Cytokine Res. 2009;29(12):817–824. PubMed PMID: 19929594.
[22] Ding S, Robek MD. Peroxisomal MAVS activates IRF1-mediated IFN-lambda production. Nat Immunol. 2014;15(8):700–701. PubMed PMID: 25045870.
[23] Zhu W, Xu J, Jiang C, et al. Pristane induces autophagy in macrophages, promoting a STAT1-IRF1-TLR3 pathway and arthritis. Clin Immunol. 2017;175:56–68. PubMed PMID: 27940139.
[24] Espert L, Rey C, Gonzalez L, et al. The exonuclease ISG20 is directly induced by synthetic dsRNA via NF-kappaB and IRF1 activation. Oncogene. 2004;23(26):4636–4640. PubMed PMID: 15064705.
[25] Dou L, Liang HF, Geller DA, et al. The regulation role of interferon regulatory factor-1 gene and clinical relevance. Hum Immunol. 2014;75(11):1110–1114. PubMed PMID: 25312803.
[26] Cadwell K. Crosstalk between autophagy and inflammatory signalling pathways: balancing defence and homeostasis. Nat Rev Immunol. 2016;16(11):661–675. PubMed PMID: 27694913.
[27] Gomes LC, Dikic I. Autophagy in antimicrobial immunity. Mol Cell. 2014;54(2):224–233. PubMed PMID: 24766886.
[28] Zhao Q, Hu ZY, Zhang JP, et al. Dual roles of two isoforms of autophagy-related gene ATG10 in HCV-subgenomic replicon mediated autophagy flux and innate immunity. Sci Rep. 2017;7 (1):11250. PubMed PMID: 28900156.
[29] Kim N, MJ K, Sung PS, et al. Interferon-inducible protein SCOTIN interferes with HCV replication through the autolysosomal degradation of NS5A. Nat Commun. 2016;7:10631. PubMed PMID: 26868272.
[30] Zhang MQ, Li JR, Peng ZG, et al. Differential effects of autophagy-related 10 protein on HCV replication and autophagy flux are mediated by its cysteine(44) and cysteine(135). Front Immunol. 2018;9:2176. PubMed PMID: 30319633.
[31] Kosugi S, Hasebe M, Entani T, et al. Design of peptide inhibitors for the importin alpha/beta nuclear import pathway by activity-based profiling. Chem Biol. 2008;15(9):940–949. PubMed PMID: 18804031.
[32] Kosugi S, Hasebe M, Tomita M, et al. Systematic identification of cell cycle-dependent yeast nucleocytoplasmic shuttling proteins by prediction of composite motifs. Proc Natl Acad Sci U S A. 2009;106(25):10171–10176. PubMed PMID: 19520826.
[33] Lee HC, Narayanan S, Park SJ, et al. Transcriptional regulation of IFN-lambda genes in hepatitis C virus-infected hepatocytes via IRF-3.IRF-7.NF-kappaB complex. J Biol Chem. 2014;289 (8):5310–5319. PubMed PMID: 24385435.
[34] Freeman BT, Sokolowski M, Roy-Engel AM, et al. Identification of charged amino acids required for nuclear localization of human L1 ORF1 protein. Mob DNA. 2019;10:20. PubMed PMID: 31080522.
[35] Nakada-Tsukui K, Watanabe N, Maehama T, et al. Phosphatidylinositol kinases and phosphatases in entamoeba histolytica. Front Cell Infect Microbiol. 2019;9:150. PubMed PMID: 31245297.
[36] Thomson SJ, Goh FG, Banks H, et al. The role of transposable elements in the regulation of IFN-lambda1 gene expression. Proc Natl Acad Sci U S A. 2009;106(28):11564–11569. PubMed PMID: 19570999.
[37] Siegel R, Eskdale J, Gallagher G. Regulation of IFN-lambda1 promoter activity (IFN-lambda1/IL-29) in human airway epithelial cells. J Immunol. 2011;187(11):5636–5644. PubMed PMID: 22058416.
[38] Ding Q, Huang B, Lu J, et al. Hepatitis C virus NS3/4A protease blocks IL-28 production. Eur J Immunol. 2012;42(9):2374–2382. PubMed PMID: 22685015.
[39] Bonjardim CA. Interferons (IFNs) are key cytokines in both innate and adaptive antiviral immune responses–and viruses counteract IFN action. Microbes Infect. 2005;7(3):569–578. PubMed PMID: 15792636.
[40] Ding CB, Zhang JP, Zhao Y, et al. Zebrafish as a potential model organism for drug test against hepatitis C virus. PLoS One. 2011;6 (8):e22921. PubMed PMID: 21857967.